Crystallization Kinetics of Poly(ethylene terephthalate) with Thermotropic Liquid Crystalline Polymer Blends

SEONG HUN KIM,[1] SANG WOOK PARK,[2] EUN SEOK GIL[1]

[1] Department of Textile Engineering, College of Engineering, Hanyang University, Seoul 133-791, Korea

[2] Technical Research Center, Dongbu Chemical, Co., Ulsan 680-110, Korea

ABSTRACT: The isothermal and dynamic crystallization behaviors of polyethylene terephthalate (PET) blended with three types of liquid crystal polymers, i.e., PHB60–PET40, HBA73–HNA27, [(PHB60–PET40)–(HBA73–HNA27) 50 : 50], have been studied using differential scanning calorimetry (DSC). The kinetics were calculated using the slope of the crystallization versus time plot, the time for 50% reduced crystallinity, the time to attain maximum rate of crystallization, and the Avrami equation. All the liquid crystalline polymer reinforcements with 10 wt % added accelerated the rate of crystallization of PET; however, the order of the acceleration effect among the liquid crystalline polymers could not be defined from the isothermal crystallization kinetics. The order of the effect for liquid crystalline polymer on the crystallization of PET is as follows: (PHB60–PET40)–(HBA73–HNA27) (50 : 50); HBA73–HNA27; PHB60–PET40: This order forms the dynamic scan of the DSC measurements. © 1998 John Wiley & Sons, Inc. J Appl Polym Sci **67:** 1383–1392, 1998

Key words: liquid crystal polymer; crystallization kinetics; poly(ethylene terephthalate; isothermal scan of differential scanning calorimetry (DSC); dynamic scan of DSC

INTRODUCTION

Poly(ethylene terephthalate) (PET) has various applications, such as in films, bottles, and fibers; recently, the focus is on the high strength polymer molecular composite to pursue stronger materials. For a reinforced PET composite, chopped glass fiber is widely used, but it makes processing difficulty because of increasing melt viscosity and decreasing rate of crystallization.[1]

Thermotropic liquid crystalline polymers (TLCPs) can provide not only improved mechanical properties to the thermoplastic matrix polymer by the formation of fibril *in situ* but also improve the processability of the polymer.[2–4]

There are many recent articles on the thermo-

tropic LCP blends. The effect of TLCP on the kinetics and thermodynamics of polymer crystallization has been also researched to define that TLCP can accelerate the rate of crystallization.[5,6] TLCPs are able to improve the mechanical property of thermoplastics as reinforcement. However, if they cause a reduction of crystallization rate, the cycle time of manufacturing the products is increased and, therefore, the productivity is decreased.

In recent articles, it is reported that an inclusion of a second TLCP in an incompatible TLCP–thermoplastic blend not only leads potentially to a ternary blend system with improved adhesion due to physical or chemical compatibilization but also provides the advantage of enhanced processability.[7]

The crystallization kinetic of PET has been investigated using differential scanning calorimetry (DSC) measurement and polarized microscopy,

---

and the crystallization study of the blend of TLCP with PET has been reported. Ou and Lin[8] and Pratt and Hobbs[9] reported the effect of PET–PHB copolyesters, which are flexible copolyesters composed of 40 mol % of PET molecular structure and show compatibility with PET, especially with the crystallization and thermal behavior of PET.

The objective of this research is to investigate the effect of the hydroxy benzoic acid–hydroxy naphthoic acid copolyester, which is a wholly aromatic TLCP and has a poor compatibility with PET, which is a semiaromatic TLCP and has a good compatibility with PET, and the effect of PET–PHB copolyester on the crystallization kinetics and thermal behaviors of PET. Furthermore, in the ternary system, which is devised for improving the adhesivity between the PET and HBA–HNA copolyester, by using the PHB–PET copolyester as a polymer coupling agent in our research group, the effect of our TLCP–TLCP blend on the crystallization kinetics and thermal property of PET is also studied.[10]

EXPERIMENTAL

Materials

The PET used in this experiment was provided by Sun Kyung Industry Co. in Korea. The wholly aromatic TLCP was obtained from Hoechst Celanese, and the semiaromatic TLCP was purchased from Unitika Ltd. The wholly aromatic TLCP is based on p-hydroxy benzoic acid (73 mol %) and 6-hydroxy-2-naphthoic acid (27 mol %) and is denoted in this article as HBA73–HNA27. The semi-aromatic TLCP is based on p-hydroxy benzoic acid (60 mol %) and ethylene terephthalate (40 mol %), and it is abbreviated as PHB60–PET40.

Preparation of Blends

All the materials were dried at 110°C *in vacuo* for at least 24 h before used. The blends were carried out by using Brabender Plasti-Corder with twin screw at the screw speed of 40 rpm and prepared in the composition of 10 wt % of TLCP in PET. PET and PHB60–PET40 were compounded at 280°C. The PET and HBA73–HNA27 binary blend and PET with HBA73–HNA27 and PHB60–PET40 ternary blend were prepared at 295°C. The ternary blend was prepared through a two-step melt blending process. Two TLCPs, PHB60–PET40 and HBA73–

HNA27, were blended at first in the proportion of 50 wt % each at 325°C. This TLCP/TLCP binary blend was extruded in Brabender and then palletized after passing the water bath. The ternary blend was then prepared by blending the ratio of 10 wt % of the binary (PHB60–PET40)–(HBA73–HNA27) blend in PET. All the PET–TLCP blends were extruded in Brabender and palletized. These pellets were dried at 110°C *in vacuo* for at least 24 h and extruded through Mini Max disc extruder for the thermal property measurements. All the samples for differential scanning calorimetry (DSC) measurements were prepared from same radius extrudates in order to achieve even thermal history.

DSC Measurement

The weight of all samples was kept in approximately 10 mg in DSC measurement by using Perkin–Elmer DSC-7. The DSC was calibrated by using 10 mg of indium. The melting temperature of indium is 156.4°C, and the indium has an enthalpy of fusion of 288.40 J/g (6.79 cal/g).

The heating and cooling scans were obtained by the following procedure. The samples were heated up to 300°C at the rate of 10°C/min under nitrogen, and the melting thermograms were recorded. At 300°C, all the samples were held for 5 min before crystallization in order to remove the previous thermal history. The crystallization thermograms were obtained by cooling the sample at the rate of 10°C/min until 20°C.

The kinetics of isothermal crystallization was measured by heating each sample to 300°C at the rate of 10°C/min, holding these for 5 min in order to remove anisotropy; then the cooling scan was performed at the rate of 200°C/min to the isothermal crystallization temperature (T_c). The corresponding crystallization exotherms scanned as a function of time until no change was observed.

THEORETICAL CONSIDERATION

In the isothermal DSC operation, the heat evolved during crystallization yields exothermic peaks, which could assist in interpreting the plot of the rate of heat evaluation, dH/dt, versus time.

The kinetic data of PET crystallization is based on the Avrami analysis. The following expression is used to measure the extent of crystallization.[10]
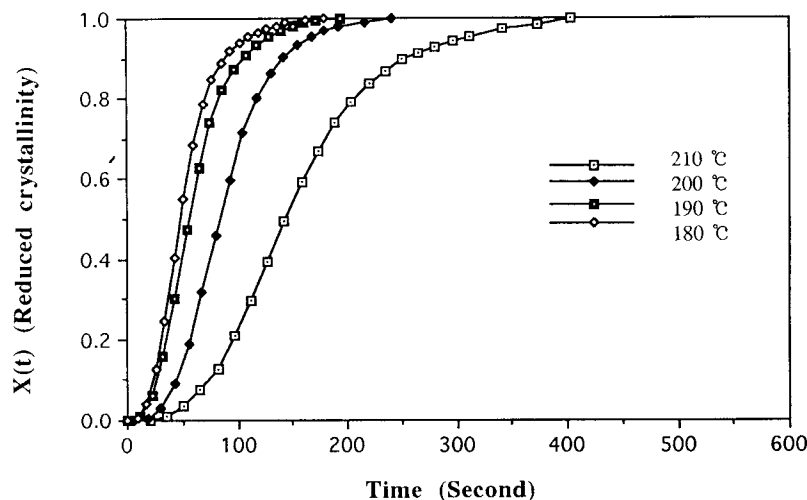
Figure 1 Reduced crystallinity of PET as a function of time.

$$X(t) = \frac{\int_0^t \frac{dH}{dt} \, dt}{\int_0^\infty \frac{dH}{dt} \, dt} \qquad (1)$$

Equating the integrals to areas of the isothermal DSC curves, eq. (1) can be shaped into

$$X(t) = \frac{A_t}{A_\infty} \qquad (2)$$

where A_t is the area under the DSC curves from $t = 0$ to $t = t$, and A_∞ is the total area under the crystallization curve. $X(\infty)$ is also called the equilibrium degree of crystallization. From this equation, the weight fraction of crystalline material $X(t)$ at a specific time can be calculated. Since any polymer can transform from amorphous to 100% crystalline, $X(t)$ is referred as the reduced crystallinity. The plots of $X(t)$ versus time for each composition and crystallization temperature T_c are shown in Figures 1–4. The induction time, τ_i, which is the distance from the thermal equilibrium point to the isotherm starting point, is found from the DSC curves. τ_i must be considered in all the isothermal DSC kinetic analysis. However, as the initiation of the exotherm does not mean that the crystalline content is zero in this moment, it must be considered that τ_i is not an exactly proper induction time. Furthermore, it may be difficult to detect the true initial point of the exotherm at the low crystallization temperature because it is difficult to attain the complete thermal equilibrium at that moment. The kinetic analysis can be

carried out using the following Avrami equation[10–12]:

$$X(t) = 1 - \exp(-kt^n) \qquad (3a)$$

where k is the rate coefficient; and n is the Avrami exponent, which is a constant that depends on both nucleation and growth of the crystals. Taking logarithms, eq. (3a) can be expressed as the following form:

$$\log[-\ln\{1 - X(t)\}] = n \log t + \log k \qquad (3b)$$

Plotting the first term versus $\log t$, both k and n could be obtained from the slope and the intercept at $\log t = 0$, respectively.

The rate coefficient can be also calculated from the half-life for the crystallization, $t_{0.5}$, by means of the following equation:

$$k' = \ln 2 / t_{0.5}^n \qquad (4)$$

T_{max} denotes the time to attain maximum rate of crystallization. The value of T_{max} can be theoretically correlated with eq. (2). When t is large and $X \neq 1$, eq. (2) can be modified to the following form:

$$\frac{X(t)}{X(\infty)} = 1 - \exp(-Kt^n) \qquad (5)$$

or

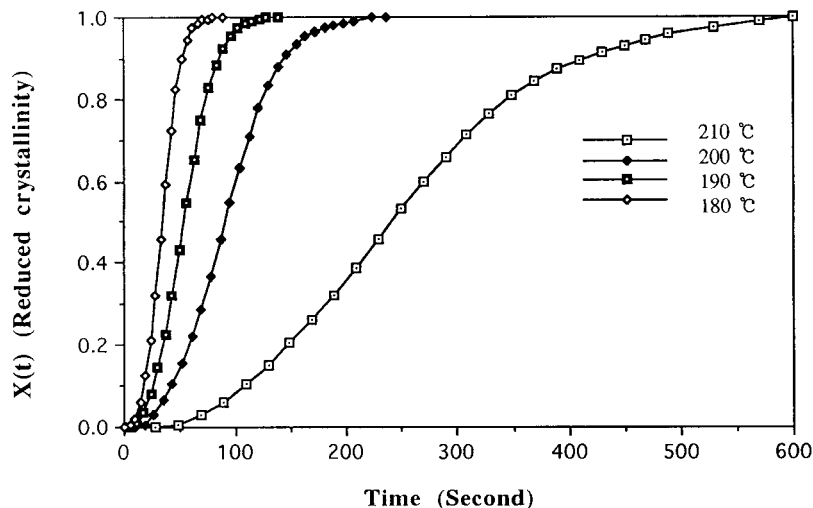$$\log\left[-\ln\left\{1 - \frac{X(t)}{X(\infty)}\right\}\right] = n \log t + \log K \qquad (6)$$

Figure 2 Reduced crystallinity as a function of time for PET−(PHB60−PET40)(90 : 10) blends.

Equation (6) can be differentiated as the following form:

$$\frac{dX(t)}{dt} = X(\infty)\, nKt^{n-1} \exp(-Kt^n) \qquad (7)$$

Then, the differentiation of eq. (7) will show

$$\frac{d^2X(t)}{dt^2} = -X(\infty)\,(-nKt^{n-1})^2 \exp(-Kt^n)$$
$$+ X(\infty)\, n(n-1)Kt^{n-2} \exp(-Kt^n) \quad (8)$$

when

$$\frac{d^2X(t)}{dt^2} = 0$$

and

$$nKt^n - (n-1) = 0$$

The time at this situation is the t_{max} in the isothermal DSC curves, as follows:

$$t_{max} = \left(\frac{n-1}{nK}\right)^{1/n} \qquad (9)$$
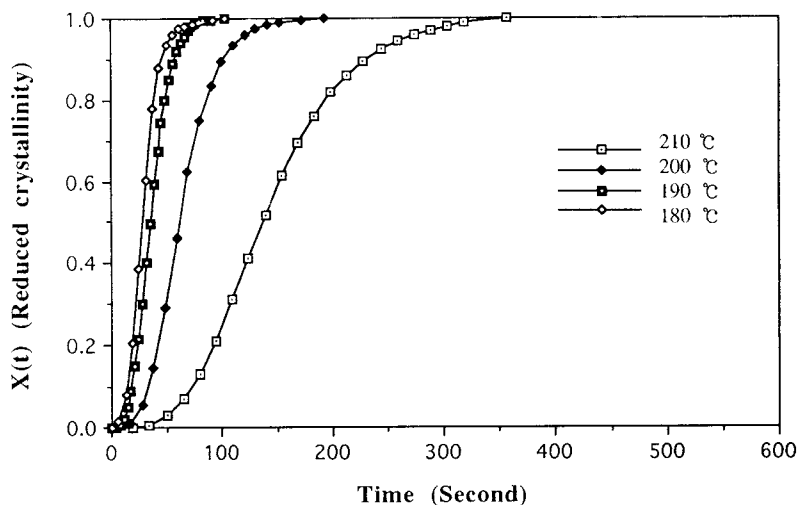
The combination of eq. (5) with eq. (9) yields

Figure 3 Reduced crystallinity as a function of time for PET−(HBA73−HNA27)(90 : 10) blends.
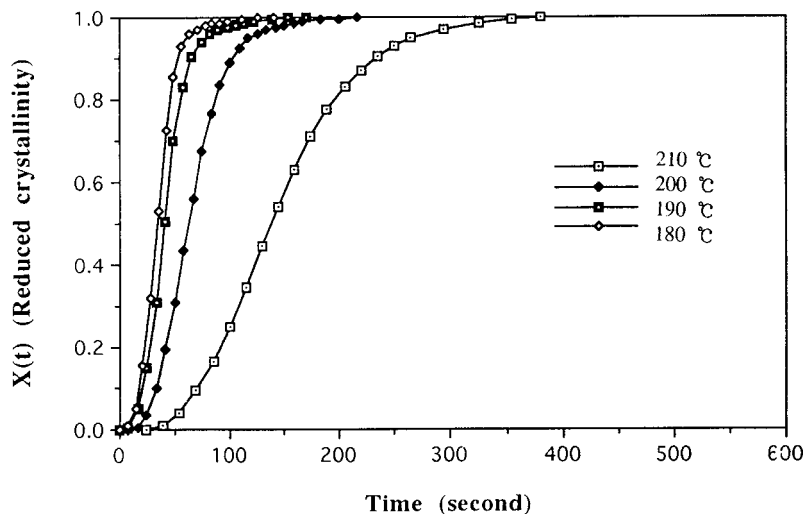
Figure 4 Reduced crystallinity as a function of time for PET–[(PHB60–PET40)–(HBA73–HNA27) 50 : 50] (90 : 10) blends.

$$\frac{X(t_{max})}{X(\infty)} = 1 - \exp\left(-\frac{n-1}{n}\right) \qquad (10)$$

where t_{max} and $X(t_{max})$ can be obtained from the DSC curves, and the Avrami exponent n^* can be calculated in eq. (10). The rate coefficient k^* can be also calculated through eq. (9).

RESULTS AND DISCUSSION

Isothermal Crystallization of PET and PET–TLCP Blends

Figure 1–4 show the plots of the reduced crystallinity versus time of PET and PET–TLCPs blends for each T_c. In the beginning of crystallization, the crystallization was shown by the delay of nucleation. After that period, the rate increased linearly until the radii of the spherulites begin to impinge on each other. As the available PET part for crystallization diminished, the slopes of curves are lowered until zero value. In addition, other parameters, $t_{0.5}$, t_{max}, and $X(t_{max})$, were determined taking the curves $X(t)$ versus t. $t_{0.5}$ is the time when the reduced crystallinity reaches the values 0.5, t_{max} is the time to attain a maximum rate of crystallization, and $X(t_{max})$ is the reduced crystallinity at t_{max}.

Figures 5–8 illustrate the plots of eq. (3b) for PET, PET–(PHB60–PET40) (90 : 10), PET–(HBA73–HNA27)(90 : 10), and PET–[(PHB60–PET40)–(HBA73–HNA27) 50 : 50] (90 : 10), respectively. The kinetic parameters, k and n, are determined in Table I for pristine PET, and Tables II–IV are for each PET–TLCPs blends. The measurements followed the Avrami equation were ranged in the midperiod of these crystallization curves, which include only the period of the primary crystallization without the secondary crystalliza-
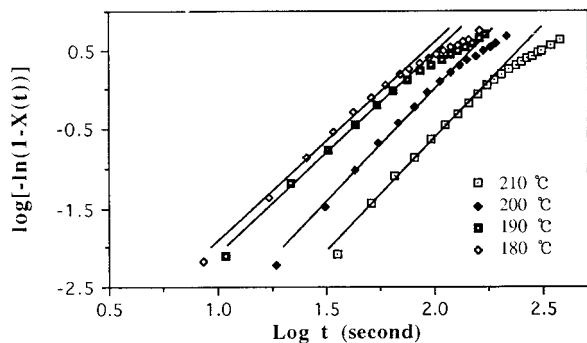

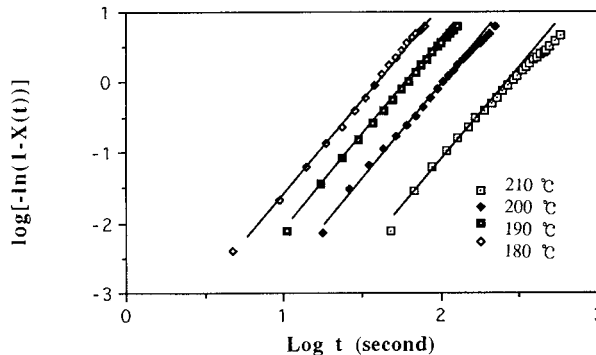**Figure 5** Avrami plot of PET at various temperatures.

Figure 6 Avrami plot of PET–(PHB60–PET40)(90 : 10) blends at various temperatures.
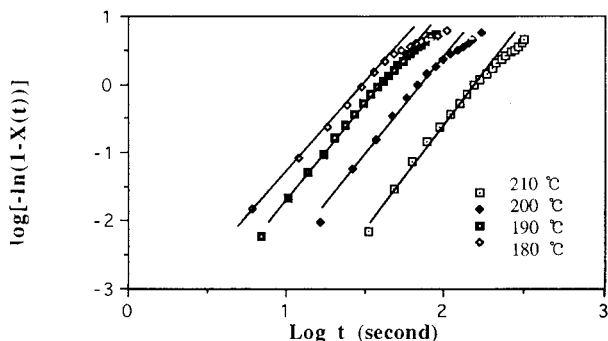
Figure 7 Avrami plots of PET–(HBA73–HNA27) (90 : 10) blends at various temperatures.

tion, because the Avrami equation assumes that the growth of crystalline ceases at the onset of the impingement between growing crystals. The rate coefficient was also calculated from the half-life of crystallization, $t_{0.5}$, using eq. (4). These results are also listed in Tables I–IV.

The rate of crystallization is strongly dependent on temperature. As temperature is decreased, the supercooling ($\Delta T = T_m^{\circ} - T_c$, where T_m° is the equilibrium melting temperature; T_c is the crystallization temperature) is increased, and the rate of crystallization increased. For example, as the crystallization temperature decreased from 210 to 200°C, the rate of crystallization of the pristine PET was increased 3.4 times. For the sample of PET–TLCPs blends, as the crystallization temperature was decreased from 210 to 200°C, the rate of crystallization was increased about 10 times.

When PHB60–PET40, HBA73–HNA27, and the 50 : 50 wt % blend of these TLCPs were blended with PET by the content of 10 wt %, all the LCPs increased the rate of crystallization of PET. This suggests that all the LCPs, PHB60–PET40, HBA73–HNA27, and (PHB60–PET40)–
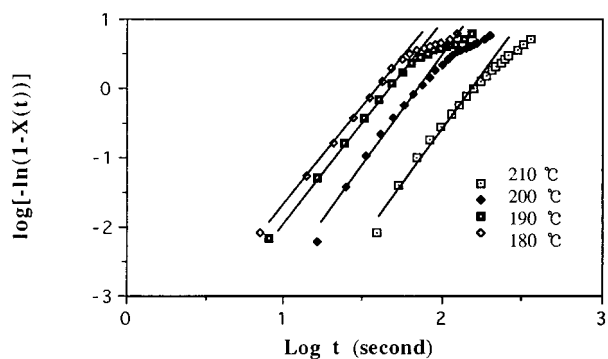

Figure 8 Avrami plots of PET–[(HBA73–HNA27)–(PHB60–PET40) 50 : 50] (90 : 10) blends at various temperatures.

Table I Isothermal Crystallization Parameters of PET

| T (°C) | PET | | | |
	k (s^{-n})	n	$t_{0.5}$ (s)	k' (s^{-n})
210	2.44×10^{-7}	3.0	143.9	2.37×10^{-7}
200	8.15×10^{-7}	3.1	84.2	8.31×10^{-7}
190	1.74×10^{-5}	2.6	55.6	1.77×10^{-5}
180	2.63×10^{-5}	2.6	48.2	2.69×10^{-5}

(HBA73–HNA27) (50 : 50), act as nucleating agents during crystallization of PET. However, it cannot be defined exactly by k and k', obtained, respectively, from the intercepts of the plots; and it is hard to define which TLCP is more effective in accelerating the rate of crystallization of PET using eq. (4). It is reported that PHB60–PET40, the flexible copolyester composed of 40 mol % of PET molecular structure, shows a compatibility with PET,[13] and that the wholly aromatic copolyester, HBA73–HNA27, has a poor adhesivity to PET.[14] However, in spite of their different molecular structures and compatibility to PET, the TLCPs as well as their blend, (PHB60–PET40)–(HBA73–HNA27) (50 : 50), all increased the rate of crystallization of PET.

As expected, the Avrami exponent is decreased as the crystallization temperature is decreased. The value of Avrami exponent n does not vary significantly with the addition of TLCPs for all the crystallization temperatures. However, as shown in Table II, the value of n of PET–(PHB60–PET40) (90 : 10) is smaller than that of PET at the crystallization temperature of 200 and 210°C; at these temperatures, n of PET exhibits 3.1 and 3.0, and n of PET–(PHB60–PET40) (90 : 10) shows 2.6 and 2.7, respectively.

For the crystallization of PET, superposing of three-dimensional growth, and dependence on ho-

Table II Isothermal Crystallization Parameters of PET–(PHB60–PET40) (90 : 10) Blend

| T (°C) | PET–(PHB60–PET 60) (90 : 10) | | | |
	k (s^{-n})	n	$t_{0.5}$ (s)	k' (s^{-n})
210	3.31×10^{-7}	2.7	241.0	2.95×10^{-7}
200	4.79×10^{-7}	2.6	90.3	4.66×10^{-6}
190	2.42×10^{-5}	2.6	53.5	2.41×10^{-5}
180	6.39×10^{-5}	2.6	34.4	6.65×10^{-5}

Table III Isothermal Crystallization Parameters of PET–(HBA73–HNA27) (90 : 10) Blends

T (°C)	k (s^{-n})	n	$t_{0.5}$ (s)	k' (s^{-n})
	PET–(HBA73–HNA 23) (90 : 10)			
210	3.79×10^{-7}	2.9	136.8	3.69×10^{-7}
200	3.24×10^{-6}	3.0	60.8	3.34×10^{-6}
190	4.27×10^{-5}	2.7	34.7	5.12×10^{-5}
180	1.39×10^{-4}	2.6	27.7	1.37×10^{-5}

mogeneous nucleation, the Avrami exponent is 4. For theoretical interpretation, the value of n is usually the integer value; but in this experiment, the n values are noninteger. However, almost all the polymers such as polyethylene,[15] poly(ethylene oxide),[16] poly(ether ether ketone),[17] and poly-(decamethylene terephthalate),[18] do not have an integer value of n. This indicates that the single nucleation mechanism does not usually happen and that the heterogeneous nucleation and the homogeneous nucleation are generated simultaneously and consecutively as the actual situation.

Table V shows k^* and n^*, which are the rate of the crystallization and the Avrami exponent calculated from eqs. (9) and (10). The t_{max} and $X(t_{max})$ can be obtained from the DSC curves. It is reported that in the experiments of the isothermal crystallization, the minimum value of t_{max} for the PET of all the molecular weights exists at around 175°C. In this research, as expected, t_{max} was decreased, as the crystallization temperature decreased from 210 to 180°C; i.e. probably as the crystallization temperature approximated to around 175°C. The dependence of t_{max} on the isothermal crystallization temperature for PET and PET/TLCPs blends is shown in Figure 9. The Avrami exponents n^*, calculated from eq. (10), range from 2.49 to 2.78, which shows lower values than the values of n to be obtained from the plots of $\log[-\ln\{1 - X(t)\}]$ versus $\log t$, which range from 2.6 to 3.1. The rate coefficient k^*, calculated from eq. (9), also increased as the crystallization temperature decreased. Except for the k^* value of PHB60–PET40 (90 : 10) at T_c = 210°C, for all of the crystallization temperatures, the rate coefficients k^*s of PET–TLCPs blends are higher than those of PET.

Dynamic Crystallization of PET and PET–TLCP blends

Figures 10 and 11 illustrate the results of DSC heating and cooling thermograms for PET, PET–

(PHB60–PET40) (90 : 10), PET–(HBA72–HNA27) (90 : 10), and PET–[(PHB60–PET40)–(HBA73–HNA27) 50 : 50] (90 : 10). Tables VI and VII shows the various parameters determined from these heating and cooling thermograms, respectively. These DSC heating thermograms exhibits a glass transition temperature T_g, a recrystallization exothermic peak, and a melting endothermic peak; and, in the cooling thermograms, there is only a distinct crystallization exothermic peak. As all the PET–TLCPs (90 : 10) blends contain just 0.9 weight fraction of the total weight fraction of sample as the fraction of PET, areas of peaks, (i.e., heat of fusion ΔH_f; heat of recrystallization ΔH_{rc}, and heat of crystallization ΔH_c) must be corrected to be compared to these of PET. The corrected enthalpy of PET–TLCPs blends was abbreviated as follows: ΔH_fPET, ΔH_{rc}PET, and ΔH_cPET. The corrected enthalpies are used for the real comparison. The melting temperatures do not change significantly between PET and PET–TLCPs blends; all the T_ms of the samples are around 252°C. The corrected heat of fusion ΔH_fPET of PET–TLCPs are increased as compared to that of PET: i.e., ΔH_fPET of PET–(PHB60–PET40) (90 : 10) and PET–(HBA72–HNA27) (90 : 10) is about 6.5 J/g higher; and ΔH_fPET of PET–[(PHB60–PET40)–(HBA73–HNA27) 50 : 50] (90 : 10) is 13.6 J/g higher than that of PET. The heat of fusion means the total crystallinity, which is the sum of primary crystallinity and secondary crystallinity. In addition, the heat of recrystallization means secondary crystallinity; then the difference between the heat of fusion and the heat of recrystallization ($\Delta H_f - \Delta H_{rc}$) can be estimated by primary crystallinity. The corrected primary crystallinity, $\Delta H_{f\text{PET}} - \Delta H_{rc\text{PET}}$ of each binary blends is about 8 J/g higher and 16.1 J/g higher than that of PET showing 13.2 J/g. As shown in Table V, the recrystallization temperature T_{rc} of PET–

Table IV Isothermal Crystallization Parameters of PET–[(HBA73–HNA27)–(PHB60–PET40) 50 : 50] (90 : 10) Blend

| T (°C)	k (s^{-n})	n	$t_{0.5}$ (s)	k' (s^{-n})
	PET–[(HBA73–HNA27)–(PHB60–PET 40) 50 : 50] (90 : 10)			
210	2.92×10^{-7}	2.6	137.9	2.76×10^{-7}
200	2.99×10^{-6}	2.6	62.5	3.03×10^{-6}
190	4.42×10^{-5}	3.0	40.4	4.03×10^{-5}
180	5.52×10^{-5}	3.0	33.9	7.38×10^{-5}

Table V   Isothermal Crystallization Parameters of PET and PET–TLCPs Blends Calculated from Eqs. (9) and (10)

| Materials	T_c (°C)	T_{max}	$n*$	$k*$
PET	210	139.3	2.8	6.95×10^{-7}
PET	200	81.0	2.6	5.90×10^{-6}
PET	190	53.1	2.6	1.79×10^{-5}
PET	180	45.0	2.5	4.63×10^{-5}
PET–(PHB60–PET40) (90 : 10)	210	232.0	2.7	2.11×10^{-7}
PET–(PHB60–PET40) (90 : 10)	200	86.1	2.6	5.03×10^{-6}
PET–(PHB60–PET40) (90 : 10)	190	50.6	2.6	2.57×10^{-5}
PET–(PHB60–PET40) (90 : 10)	180	32.9	2.6	7.46×10^{-5}
PET–(HBA72–HNA27) (90 : 10)	210	132.0	2.7	1.05×10^{-6}
PET–(HBA72–HNA27) (90 : 10)	200	58.8	2.6	1.01×10^{-5}
PET–(HBA72–HNA27) (90 : 10)	190	33.0	2.6	7.70×10^{-5}
PET–(HBA72–HNA27) (90 : 10)	180	27.0	2.6	1.15×10^{-4}
PET–[(HBA73–HNA27)–(PHB60–PET40) 50 : 50] (90 : 10)	210	133.0	2.8	9.06×10^{-7}
PET–[(HBA73–HNA27)–(PHB60–PET40) 50 : 50] (90 : 10)	200	59.4	2.6	1.70×10^{-5}
PET–[(HBA73–HNA27)–(PHB60–PET40) 50 : 50] (90 : 10)	190	38.0	2.5	7.04×10^{-5}
PET–[(HBA73–HNA27)–(PHB60–PET40) 50 : 50] (90 : 10)	180	32.0	2.6	8.66×10^{-5}

TLCPs blends are decreased by 2–3°C, and ΔT_{rc} of PET–TLCPs is narrowed as compared to the parameters of PET. TLCPs increase the crystallization temperature T_c and decrease ΔT_c of PET. The crystallization peak of PET–[(PHB60–PET40)–(HBA73–HNA27) 50 : 50] (90 : 10) ex-hibits the most deviation from the crystallization peak of PET.

These results suggest that two TLCP and their TLCP–TLCP blends act as the nucleating agents for the crystallization of PET. This result is con-

Figure 9 The time necessary to attain a maximum rate of crystallization of PET and PET–TLCPs blends.
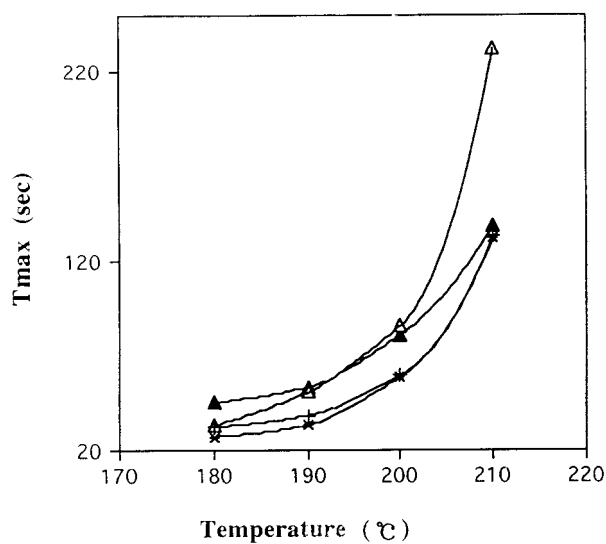
Legend:
- ▲ PET
- △ PET/(PHB60/PET40) (90/10)
- ✕ PET/(HBA73/HNA27) (90/10)
- + PET/[(PHB60/PET40)/(HBA73/HNA27) 50/50] (90/10)
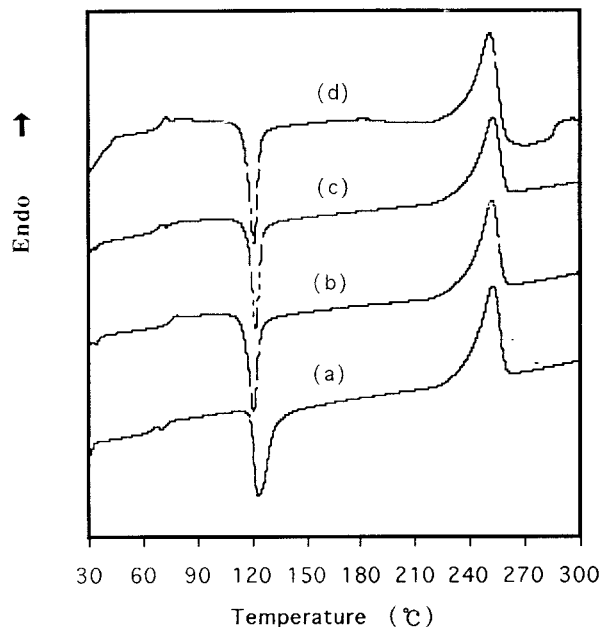
Figure 10 DSC thermogram of PET and PET–LCP blends (heating rate is 10°C/min under nitrogen): (a) PET, (b) PET–(PHB60–PET40) 90 : 10, (c) PET–(HBA73–HNA23) 90 : 10, and (d) PET–[(HBA73–HNA27)–(PHB60–PET40) 50 : 50] 90 : 10.
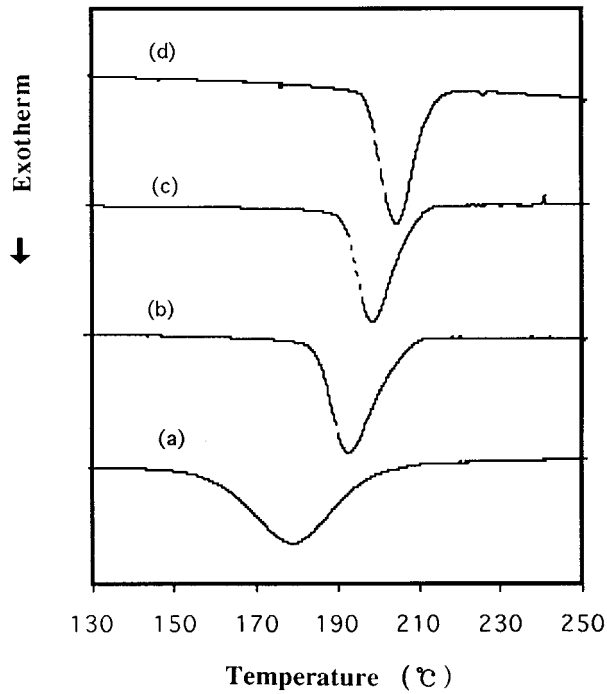
Figure 11 DSC thermogram of PET and PET–LCP Blends from cooling (cooling rate is 10°C/min under nitrogen): (a) PET, (b) PET–(PHB60–PET40) 90 : 10, (c) PET–(HBA73–HNA23) 90 : 10, and (d) PET–[(HBA73–HNA27)–(PHB60–PET40) 50 : 50] 90 : 10.

sistent with that obtained from the isothermal crystallization experiment.

The values listed in Tables VI and VII illustrate that ΔH_f PET $-$ ΔH_{rc} PET and ΔH_f PET of PET–[(PHB60–PET40)–(HBA73–HNA27) 50 : 50] (90 : 10) are largest in those of PET and PET–TLCPs blends, and those values of PET–(PHB60–PET40) (90 : 10) and PET–(HBA72–HNA27) (90 : 10) are almost the same. In addition, PET–[(PHB60–PET40)–(HBA73–HNA27) 50 : 50] (90 : 10) exhibits the highest value of T_c and the smallest value of ΔT_c in those of PET and PET–TLCPs blends, and PET–(HBA72–HNA27) (90 : 10) has the higher value of T_c and the smaller value of ΔT_c than those values of PET–(PHB60–PET40) (90 : 10). The higher the value of T_c the higher the rate of crystallization; the smaller the value of ΔT_c, the higher the rate of crystallization. These results are attributed to the fact that PET–[(PHB60–PET40)–(HBA73–HNA27) 50 : 50] (90 : 10) accelerates the crystallization rate of PET most significantly, and HBA73–HNA27 affects the crystallization of PET more than PHB60–PET40.

CONCLUSION

The effect of thermotropic liquid crystalline polymers on the crystallization of PET has been inves-

Table VI   DSC Data of PET and PET–TLCPs Blends from Heating Scan (10°C/min)

Materials	Recrystallization					Melting					Difference	
	Onset (°C)	T_{rc} (°C)	ΔT_{rc} (°C)	ΔH_{rc} (J/g)	ΔH_{rc} PET (J/g)	Onset (°C)	T_m (°C)	ΔT_m (°C)	ΔH_f (J/g)	ΔH_f PET (J/g)	$\Delta H_f - \Delta H_{rc}$ (J/g)	ΔH_f PET and ΔH_{rc} PET
PET	118.6	123	43	28.9	28.9	239	252	45.5	42.3	42.1	13.4	13.2
PET–(PHB60–PET40) (90 : 10)	114.5	120	35	24.8	27.6	239	252	45.8	43.8	48.7	19	21.1
PET–(HBA 73–HNA27) (90 : 10)	116.7	121	29	24.6	27.3	239	252	45.8	43.7	48.6	19.1	21.3
PET–[(HBA73–HNA27)–(PHB60–PET40) 50 : 50] (90 : 10)	115	120	30.4	23.8	26.4	237	251	48.1	50.1	55.7	26.3	29.3

Table VII   DSC Data of PET and PET–LCP Blends from Cooling Scan (10°C/min)

Material	Crystallization				
	Onset (°C)	T_c (°C)	ΔT_c (°C)	ΔH_c (J/g)	ΔH_c PET (J/g)
PET	196.2	179.2	75.9	40.7	40.7
PET–PHB60–PET40 (90 : 10)	205.2	192.8	42.7	41.0	45.6
PET–HBA73–HNA27 (90 : 10)	208.6	198.6	38.6	40.1	44.6
PET–[(HBA73–HNA27)–(PHB60– PET40) 50 : 50] (90 : 10)	212.5	204.5	37.5	40.6	45.1

tigated by the isothermal and the dynamic procedure of DSC.

In the isothermal crystallization DSC scans, the kinetics of the crystallization process was described by the Avrami equation. When PHB60–PET40, HBA73–HNA27, and the 50 : 50 wt % blend of these TLCPs were blended with PET by the content of 10 wt %, all of them increased the rate of crystallization of PET. The rate coefficient k^* is increased, and $t_{\max}$ is decreased as the crystallization temperature is decreased from 210 to 180°C.

In the heating and the cooling DSC scans, all the TLCPs increase ΔH_fPET, ΔH_{rc}PET $- \Delta H_{rc}$PET, and T_c and decrease ΔT_c, showing that TLCPs assist the crystallization of PET.

It cannot be exactly defined which TLCP or binary blended TLCP more greatly accelerate the rate of crystallization of PET from the isothermal crystallization kinetics (showing almost similar effects); but in the data of thermograms, the effects were the strongest for PET–[(PHB60–PET40)–(HBA73–HNA27) 50 : 50] (90 : 10), and HBA73–HNA27 has a tendency of improving the crystallization of PET more than PHB60–PET40 from the thermograms.

REFERENCES

1. S. Cheng and R. A. Shanks, *J. Appl. Polym. Sci.,* **47,** 2149 (1993).
2. W. Lee and A. T. DiBenedetto, *Polymer,* **34,** 684 (1993).
3. S. S. Bafna, T. Sun, and D. G. Baird, *Polymer,* **34,** 708 (1993).
4. A. Datta and Donard. G. Baird, *Polymer,* **36,** 505 (1995).
5. S. K. Battacharya, A. Tendolkar, and A. Misra, *Mol. Cryst. Liq. Cryst.,* **153,** 501 (1987).
6. S. K. Sharma, A. Tendolkar, and A. Misra, *Mol. Cryst. Liq. Cryst., Inc. Nonlin. Opt.,* **157,** 597 (1988).
7. W. C. Lee and A. T. Dibenedetto, *Polym. Eng. Sci.,* **32,** 400 (1992).
8. C. F. Ou and C. C. Lin, *J. Appl. Polym. Sci.,* **54,** 1223 (1994).
9. C. F. Pratt and S. Y. Hobbs, *Polymer,* **17,** 12 (1976).
10. P. C. Vilanova, S. M. Ribas, and G. M. Guzman, *Polymer,* **26,** 423 (1985).
11. M. Avrami, *J. Chem. Phys.,* **7,** 1103 (1939).
12. M. Avrami, *J. Chem. Phys.,* **9,** 117 (1941).
13. P. Zhuang, T. Kyu, and J. L. White, *Polym. Eng. Sci.,* **28,** 1095 (1988).
14. W. N. Kim and M. M. Denn, *J. Rheol.,* **36,** 1477 (1992).
15. W. Banks, M. Gorden, R. J. Roe, and A. Sharples, *Polymer,* **4,** 61 (1963).
16. Yu. Godovsky, G. L. Slonimsky, and N. M. Garbar, *J. Polym. Sci., Polym. Symp.,* **37,** 1 (1972).
17. I. J. Hiller, *J. Polym. Sci.,* **3,** 3067 (1965).
18. A. Sharples and E. L. Swinton, *Polymer,* **4,** 119 (1963).